



Faculty of Mechanical Engineering

**MODELLING THE ACOUSTIC PERFORMANCE OF
INHOMOGENEOUS MICRO-PERFORATED PANEL ABSORBER**

Ali Ibrahim Mosa

Doctor of Philosophy

2021

**MODELLING THE ACOUSTIC PERFORMANCE OF INHOMOGENEOUS
MICRO-PERFORATED PANEL ABSORBER**

ALI IBRAHIM MOSA

**A thesis submitted
in fulfilment of the requirements for the degree of Doctor of Philosophy**

Faculty of Mechanical Engineering

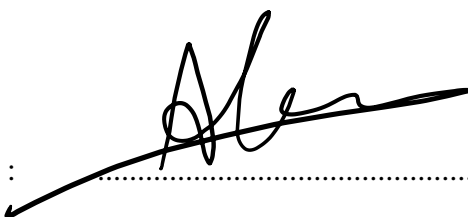
UNIVERSITI TEKNIKAL MALAYSIA MELAKA

2021

DECLARATION

I declare that this thesis entitled “Modelling the Acoustic Performance of Inhomogeneous Micro-Perforated Panel Absorber” is the result of my research except as cited in the references. The thesis has not been accepted for any degree and is not concurrently submitted in the candidature of any other degree.

Signature

: 

Name

: Ali Ibrahim Mosa

Date

: 20/1/2021

APPROVAL

I hereby declare that I have read this thesis and in my opinion this thesis is sufficient in terms of scope and quality for the award of Doctor of Philosophy.

Signature :

Supervisor Name : Associate Professor Dr. Azma Putra

Date :

DEDICATION

Dedicated to Allah S.W.T. Almighty and Rasul-Allah S.A.W. Thanks also

To the Father in My Heart,
For his prayers and care for me

To my Mother
A strong and gentle soul who taught me to trust in Allah, believes in hard work and
thought so much could be done with less

To my brother and sister
To my Wife who stands with me and supports me in all aspects of my life

To my Children
The reason of what I have become today
Thanks for your wholehearted support and continuous care

ABSTRACT

Micro-perforated panel (MPP) absorber is increasingly gaining more popularity in noise control as a sound absorber given its facile installation, long durability, environmental friendliness and attractive appearance and as an alternative to the classical porous acoustics materials. A single MPP absorber typically features a Helmholtz resonator with a high absorption amplitude, but narrow absorption bandwidth. The main objective of this study is to obtain a wider sound absorption bandwidth by proposing an inhomogeneous perforation technique. The first step is to study the acoustic performance of a single layer MPP containing holes of two different sizes and ratios and with multiple cavity depths. Thereafter, for more improvement of the absorption bandwidth, this single MPP is cascaded with another single MPP to form a double-layer MPP model of inhomogeneous perforation. Mathematical models based on the equivalent electrical circuit method are proposed, and the absorption coefficient is calculated under a normal incidence of sound. The results show that the introduction of inhomogeneous perforation technique improves the absorption performance of the single layer MPP absorber compared to the homogenous one, especially with multi-cavity depths. The MPP layer should consist of two sets of perforation parameters set in an equal arrangement in two sub MPP areas; one of smaller perforation ratio with large hole diameter and the other of larger perforation ratio with smaller hole diameter. The proposed double layer inhomogeneous MPP model exhibits significantly wider sound absorption bandwidth and higher sound absorption amplitude than that of the conventional double-layer and even triple-layer homogeneous MPPs. The results demonstrate that the absorption bandwidth can be effectively controlled to higher frequencies region by reducing the air cavity between the two inhomogeneous MPP layers, and by decreasing the cavity depth behind the sub-MPP with small hole diameter and high perforation ratio. For the low frequency improvement, this can be achieved by increasing the cavity depth behind the sub-MPP with large hole diameter-small perforation ratio. The theoretical results were validated with the experiments by using the impedance tube method with a good agreement. This study also presents an empirical mathematical model for the single layer, multi cavity inhomogeneous MPP to conveniently obtain the required MPP parameters to have the half-absorption bandwidth of absorption coefficient.

PEMODELAN PRESTASI AKUSTIK DARI PANEL PENYERAP BERTEBUK-MIKRO TIDAK SERAGAM

ABSTRAK

Penyerap panel bertebuk-mikro (MPP) menjadi semakin popular dalam kawalan bunyi disebabkan pemasangannya yang mudah, tahan lama, mesra alam dan mempunyai rupa yang menarik serta sebagai alternatif kepada bahan penyerap akustik berliang klasik. Penyerap MPP tunggal biasanya mempunyai ciri-ciri tipikal seperti penyalun Helmholtz dengan amplitud penyerapan tinggi, tetapi dengan lebar jalur penyerapan yang sempit. Objektif utama kajian ini adalah bagi mendapatkan lebar jalur penyerapan bunyi lebih besar dengan mencadangkan teknik tebukkan tak homogen. Langkah pertama adalah untuk mengkaji prestasi panel bertebuk-mikro tunggal yang mempunyai dua saiz dan nisbah lubang yang berlainan dan pelbagai kedalaman rongga. Selepas itu, untuk meningkatkan jalur penyerapan, MPP tunggal ini disusun dengan satu lagi MPP tunggal untuk membentuk model dua lapisan MPP bertebuk tak homogen. Model matematik yang dicadangkan adalah berdasarkan model litar elektrik setara dan pekali penyerapan dikira pada bunyi tuju normal. Hasil kajian menunjukkan pengenalan teknik tebukkan tak homogen meningkatkan prestasi penyerapan lapisan MPP tunggal berbanding dengan teknik homogen, terutamanya dengan pelbagai kedalaman rongga. Lapisan MPP hendaklah terdiri daripada dua set parameter tebukkan yang ditetapkan pada susunan sama dalam dua kawasan sub MPP, satu nisbah tebukkan sedikit dengan diameter lubang besar dan satu lagi bernisbah tebukkan lebih banyak dengan diameter lubang kecil. Model dua lapisan MPP tak homogen yang dicadangkan mempamerkan kelebaran jalur penyerapan yang lebih ketara dan amplitud penyerapan tinggi berbanding dengan dua-lapisan dan tiga-lapisan MPP homogen konvensional. Hasil kajian menunjukkan bahawa jalur penyerapan dikawal secara efektif ke frekuensi tinggi dengan mengurangkan rongga udara di antara dua lapisan MPP tak homogen, dan dengan mengurangkan kedalaman rongga di bahagian belakang sub-MPP berdiameter kecil dan tebukkan bernisbah tinggi. Bagi menambah baik frekuensi rendah, kedalaman rongga di belakang sub-MPP dengan diameter lubang besar-bernisbah tebukkan sedikit ditingkatkan. Hasil teori disahkan dengan eksperimen menggunakan kaedah tiub impedans menunjukkan hasil yang baik. Kajian ini juga menunjukkan model matematik empirik bagi MPP tunggal, pelbagai kedalaman rongga MPP tak homogen digunapakai untuk mendapatkan parameter MPP yang diperlukan bagi mencapai separuh-jalur penyerapan daripada pekali penyerapan.

ACKNOWLEDGEMENTS

Alhamdulillah, first and foremost, I would like to praise to Allah S.W.T, the Almighty for giving me a little strength and granting me the capability to do my thesis. Heartiest gratitude to my supervisors: Associate Professor Dr. Azma Putra and Associate Professor Dr. Roszaidi bin Ramlan for their kind advice, guidance, encouragements, and supports during my doctoral research and study. The achievements and completion of the thesis will be very hard to be possible without their valuable, sincere and relentless supervision. I would like to thank my family, especially to my wife, and my children for their great support and encourage. Throughout my doctoral research, there have been supporting and assistance of several people who helped me to finish this research. Therefore, it is an opportunity to thank and appreciate these people's great efforts. I want to express my thanks to Mr. Johardi, from the laboratory vibro-acoustic in Faculty of Mechanical Engineering (FKM), for his assistance, time and efforts during the measurement and fabrication. To all my colleagues and fellow friends, especially Dr. Osam H. Attia from the University of Baghdad, I would like to express my thanks for their support. Last, thank you to everyone who supported me directly or indirectly and always remember me and praying for my success. Thank you very much.

TABLE OF CONTENTS

	PAGE
DECLARATION	
APPROVAL	
DEDICATION	
ABSTRACT	i
ABSTRAK	ii
ACKNOWLEDGEMENTS	iii
TABLE OF CONTENTS	iv
LIST OF TABLES	viii
LIST OF FIGURES	x
LIST OF APPENDICES	xxii
LIST OF ABBREVIATIONS	xxiii
LIST OF NOMENCLATURES	xxv
LIST OF CONSTANTS	xxvii
LIST OF PUBLICATIONS	xxviii
CHAPTER	
1. INTRODUCTION	1
1.1 Background of the study	1
1.2 Problem statement	5
1.3 Main aim of the study	7
1.4 Objectives of the study	7
1.5 Scopes and limitations of the study	7
1.6 General methodology	8
1.6 Thesis outline	11
1.7 Thesis contributions	12
2. LITERATURE REVIEW	14
2.1 Introduction	14
2.2 MPP physical parameters	16
2.2.1 The thickness of the panel	16
2.2.2 Hole diameter	16
2.2.3 Hole space	16
2.2.4 Perforation ratio	17
2.2.5 Air-cavity depth	17
2.3 Acoustic impedance of Maa model	17
2.4 Sound absorption coefficient	19
2.5 Single-layer microperforated panel sound absorber (SL-MPP)	20
2.5.1 Single-layer MPP sound absorber with a porous material	20
2.5.2 Flexible single layer MPP sound absorber	22
2.5.3 Single-layer MPP sound absorber with modifications of the back air-cavity	24
2.5.4 Single-layer MPP sound absorber with ultra-hole size	25
2.5.5 Single-layer MPP sound absorber with multi-cavity depth	26

2.5.6	Three-dimensional single layer MPP space sound absorbers	27
2.6	Multilayer MPP sound absorber	28
2.6.1	Multi-layer MPP sound absorber in a series arrangement	29
2.6.1.1	Multi-Layer MPPs with a porous material	34
2.6.1.2	Flexible multi-layer MPPs sound absorber	35
2.6.1.3	Multi layer MPP sound absorber with modifications of the backed air-cavity	38
2.6.1.4	Multi layer MPP sound absorber with multi-cavity depth	38
2.6.1.5	Three-dimensional multi-layer MPP space sound absorbers	40
2.6.1.6	Transparent multi-layer MPP sound absorbers	40
2.6.2	Multiple MPPs sound absorber in a parallel arrangement	41
2.6.2.1	Multiple MPPs in a parallel arrangement with uniform cavity depth	41
2.6.2.2	Multiple MPPs in a parallel arrangement with multi cavity depth	47
2.7	Theoretical calculations methods	48
2.8	Impedance tube method	50
2.9	Design of experiments	51
2.9.1	Response Surface Methodology (RSM)	51
2.9.2	Central Composite Design (CCD)	54
2.10	Critical discussions	55
2.11	Summary	59
3.	RESEARCH METHODOLOGY	60
3.1	Introduction	60
3.2	Single-Layer inhomogeneous micro-perforated panel model (SL-iMPP)	64
3.3	SL-iMPP with a multi-cavity depth mathematical model	65
3.3.1	Acoustic impedance and absorption coefficient of SL-iMPP	66
3.3.2	Numerical analysis predictions set up	69
3.3.3	Theoretical validation	69
3.3.4	Experimental validation	70
3.3.4.1	Modelling of SL-iMPP system using SolidWorks software	70
3.3.4.2	Materials	73
3.3.4.3	Samples fabrication	73
3.3.4.4	Experimental setup and absorption coefficient measurement	76
3.3.4.5	Range of the valid frequency	80
3.4	Double Layer Inhomogeneous Micro-Perforated Panel model (DL-iMPP)	82
3.4.1	DL-iMPP absorber with a uniform air cavity	83
3.4.1.1	Back air cavity with partition model	84
3.4.1.2	Back air cavity without partition model	88
3.4.2	DL-iMPP absorber with multiple back cavity depth	90

3.4.3	Model validation	94
3.4.3.1	Parameters	94
3.4.3.2	Modelling using SolidWorks	95
3.4.3.3	Materials	100
3.4.3.4	Samples fabrication	100
3.4.3.5	Experimental setup and absorption coefficient measurement	101
3.5	Design of Experiment (DoE)	103
3.5.1	Utilisation of response surface methodology	106
3.5.2	Central composite design	107
3.6	Summary	111
4.	RESULT AND DISCUSSION	113
4.1	Introduction	113
4.2	Results of the theoretical validation	115
4.3	Single-layer inhomogeneous MPP absorber (SL-iMPP)	118
4.3.1	Parametric study	118
4.3.1.1	Effect of inhomogeneous pattern	118
4.3.1.2	Effect of perforation ratio	121
4.3.1.3	Effect of hole diameter	125
4.3.1.4	Effect of panel thickness	128
4.3.1.5	Effect of back cavity depth	131
4.3.2	Measured absorption coefficient and model validation	134
4.3.3	Summary	138
4.4	Double-layer inhomogeneous MPP absorber (DL-iMPP)	138
4.4.1	DL-iMPP with a uniform cavity depth	138
4.4.1.1	Case with and without the cavity partition	138
4.4.1.2	Comparison of SL-iMPP and DL-iMPP	144
4.4.1.3	Comparison of DL-iMPP and DL-MPP	146
4.4.1.4	Effect of cavity depth	150
4.4.1.5	Summary	152
4.4.2	DL-iMPP with multiple-cavity depths	152
4.4.2.1	Comparison with other MPP systems	153
4.4.2.2	Effect of multiple-cavity depths	158
4.4.3	Measured absorption coefficient and model validation	163
4.4.3.1	Measured absorption coefficient of DL-iMPP	163
4.4.3.2	Measured absorption coefficient of DL-iMPP _{MD}	167
4.4.3.3	Summary	175
4.5	Empirical model	176
4.5.1	Response Surface Methodology (RSM) and the statistical analysis	176
4.5.2	Analysis of variance (ANOVA) and multiple regression analysis	177
4.5.3	Effect of tested parameters of the SL-iMPP on absorption coefficient (alpha)	183
4.5.3.1	Selection of the perforation ratio	183
4.5.3.2	Selection of the holes size	185
4.5.3.3	Selection of the back cavity depths	187
4.5.3.4	Summary	189

5. CONCLUSION AND RECOMMENDATION FOR FUTURE WORKS	190
5.1 Conclusion	190
5.2 Limitation and recommendations for future work	192
REFERENCES	194
APPENDICES	207

LIST OF TABLES

TABLE	TITLE	PAGE
2.1	Micro-perforated panels (MPP) absorber structure technique	58
3.1	PVC inhomogeneous MPPs absorbers samples structural parameters	71
3.2	List of the equipment used in impedance tube apparatus	76
3.3	Range of structural parameters for the DL-iMPP _{MD} system	94
3.4	Inhomogeneous MPPs absorbers model structural parameters	96
3.5	Design range for the input parameters (independent variables) of the SL-iMPP model	108
3.6	Design matrix of the analysis of variance for the response (sound absorption coefficient)	109
4.1	Structural parameters of SL-iMPP and DL-iMPP	144
4.2	Structural parameters of the double-layer homogeneous MPP (DL-MPP) and double layer inhomogeneous MPP (DL-iMPP)	148
4.3	Structural parameters SL-MPP, DL-MPP, TL-MPP and the DL-iMPP system	153
4.4	Structural parameters of DL-MPP and DL-iMPP _{MD}	155
4.5	Half-power absorption bandwidth, Δf for various MPP models	157

4.6	Central Composite Design (CCD) for the sound absorption coefficient of SL-iMPP	177
4.7	Analysis of variance ANOVA for Response Surface Reduced Quadratic model	179
4.8	Central Composite Design (CCD) for the absorption coefficient of SL-iMPP	181
4.9	Summary of sound absorption performance of the SL-MPP obtained from the two design points A and B as in Figure 4.40	185

LIST OF FIGURES

FIGURE	TITLE	PAGE
1.1	Schematic diagram of single layer micro-perforated panel (MPP) absorber (Maa, 1975)	3
1.2	Use of MPP absorbers in multiple noise control applications, (a) MRI (Li and Mechefske, 2010a), (b) building acoustics (Helmut et. al., 2006), (c) electrical transformers (Liu et al., 2016), (d) Muffler system (Chihua et al., 2019)	5
1.3	Thesis overview flow chart	10
2.1	Flowchart of the classification of micro-perforated panel absorber models techniques	15
2.2	Electrical equivalent circuit for single layer MPP (Maa, 1975)	18
2.3	Schematic diagram of single layer micro-perforated panel combined with a porous absorber (Liu et al., 2017a)	21
2.4	Single-layer MPP absorber with a honeycomb structure in the back air cavity (Yang and Cheng, 2016)	23
2.5	Schematic diagram of a single-layer MPP absorber combined with a parallel-arranged tube structure (Li et al., 2016)	23
2.6	Photo of single-layer MPP absorber model with ultra-micro hole size (Qian et al., 2013)	26

2.7	Single-layer MPP absorbers with different air-cavity depths (Min and Guo, 2019)	27
2.8	Double-layer MPP absorber structure (Zhang and Gu, 1998)	31
2.9	Double-layer MPP absorber electric equivalent circuit (Zhang and Gu, 1998)	31
2.10	Schematic diagrams of triple-layer MPP (TL-MPP) (Zhu, 2011)	33
2.11	Sound absorption coefficient of multi-layer MPPs absorber system, (n: is number of MPP layers), panel thickness = 1.5 mm; hole diameter = 0.5 mm, perforation ratio = 6%, and cavity depth = 30 mm, (Bucciarelli et al., 2019)	34
2.12	Schematic diagrams of hybrid MPP absorber system include a porous-absorber-material (Cobo et al., 2010)	35
2.13	Schematic diagrams of double layer MPP absorber with a permeable membrane (PM) (Sakagami et al., 2014a)	36
2.14	Effect of a honeycomb on sound absorption performance of a DL-MPP absorber model, solid line: the model with a honeycomb, dashed line: the model without a honeycomb (Sakagami et al., 2011b)	37
2.15	Schematic diagrams of double-layer MPPs absorber model with multi cavity depths (Qian et al., 2017)	40
2.16	The sound absorption coefficient of single-layer MPP with uniform hole size and multi hole size, with a uniform cavity depth of 15 mm (Miasa et al., 2007)	42
2.17	Multi different single layer MPPs set in parallel arrangement	44

	(Sakagami et al., 2009a)	
2.18	Schematic diagram of multiple MPPs in parallel arrangement model with inhomogeneous perforation (Prasetiyo et al., 2016)	46
2.19	Impedance tube schematic drawing (Brandao et al., 2009)	50
2.20	Experimental designs for optimisation of three variables using CCD method	55
2.21	Research taxonomy chart showing thesis contribution	57
3.1	Research methodology flowchart	63
3.2	Sketch of the single-layer inhomogeneous MPP absorber model, front view	64
3.3	Schematic diagrams of the single-layer inhomogeneous MPP with a multi-cavity depth	65
3.4	Electrical equivalent circuit of: (a) traditional single layer MPP (Maa, 1975), (b) author's proposed single layer inhomogeneous MPP with multi-cavity depth model	68
3.5	Schematic diagrams of the inhomogeneous MPP absorber samples: (a) i-MPP-1; (b) i-MPP-2	71
3.6	Isometric view of SL-iMPP model parts (a) cylindrical-shaped case with a partition separating the two-cavity, (b) and (c) a two-mobile backed rigid mass	72
3.7	Inhomogeneous MPP model assembled with cylindrical-shaped case and two-mobile backed rigid mass (a) isometric view; (b) and (c) isometric cross section view	72
3.8	Photos of the manufacturing of the inhomogeneous micro-	74

	perforated panel samples	
3.9	Inhomogeneous MPP model parts, (a) i-MPP-1; (b) i-MPP-2; (c) cylindrical-shaped case; (d) two-mobile backed rigid mass	75
3.10	Devices and parts used in impedance tube apparatus as listed in Table 3.2	77
3.11	Impedance tube apparatus in laboratory	78
3.12	MPP sample inside impedance tube	79
3.13	Diagram of the experimental setup for the normal-incidence absorption coefficient measurement using the impedance tube method	80
3.14	Schematic diagram of double-layer inhomogeneous MPP absorber model	83
3.15	Schematic diagram of the double-layer inhomogeneous MPP absorber model with uniform back cavity and separated partition	85
3.16	The electrical equivalent circuit model for: (a) traditional DL-MPP system presented by Zhang and Gu (1998) and (b) author's proposed DL-iMPP model for the case where a partition separates the back cavity of the iMPP ₂	86
3.17	The simplified equivalent circuit model from that in Figure 3.16	87
3.18	Schematic diagram of the DL-iMPP system with a uniform back cavity and without separated partition	89
3.19	The electrical equivalent circuit model of the DL-iMPP system for the case where the back cavity of the iMPP ₂ is not separated by a partition	89

3.20	Double-layer inhomogeneous MPP absorber system backed with multiple-cavity depths, DL-iMPP _{MD} , (isometric view)	91
3.21	Schematic diagram of the DL-iMPP system backed with multiple-cavity depths, (DL-iMPP _{MD})	92
3.22	The electrical equivalent circuit model of the DL-iMPP _{MD}	92
3.23	Schematic diagrams of the inhomogeneous MPP absorber samples listed in Table 3.4, designed by SolidWorks	97
3.24	Schematic diagrams of the cylindrical cases of the cavities between the two iMPPs and for the back cavity behind the second layer iMPP ₂	98
3.25	Schematic diagram of the DL-iMPP model with uniform cavity depth and separated partition	99
3.26	Schematic diagram of the DL-iMPP model with uniform cavity depth and without a separated partition	99
3.27	Schematic diagram of the DL-iMPP _{MD} model (with multiple cavity depth)	100
3.28	The inhomogeneous MPP test samples and the cylindrical cases pictures, (1) iMPP ₁ , (2) iMPP ₂ , (3) iMPP ₃ , (4) iMPP ₄ , (5) iMPP ₅ , (6) iMPP ₆ , (7) iMPP ₇ , (8) cylindrical cases	101
3.29	Experimental setup for the measurement of the normal absorption coefficient of DL-iMPP absorber models	103
3.30	Flowchart of the proposed DoE methodology	105
4.1	Methodology flowchart of the simulation and experimental of iMPP results	114

4.2	Sound absorption coefficient for SL-MPP of different structural parameters: (1) $d = 0.3$ mm, $b = 2$ mm, $t = 0.4$ mm, $D = 50$ mm; (2) $d = 0.4$ mm, $b = 3.5$ mm, $t = 0.4$ mm, $D = 100$ mm; (3) $d = 0.4$ mm, $b = 4$ mm, $t = 0.4$ mm, $D = 40$ mm; (a) Maa model (Maa, 1987); (b) by author's Matlab code	116
4.3	Sound absorption coefficient for SL- MPP of different structure parameters: (case 1) $d = 0.5$ mm, $p = 1\%$, $t = 0.5$ mm, $D = (2, 20, 10, 50, 100, 25)$ mm; (case 2) $d = 0.5$ mm, $p= 1\%$, $t = 0.5$ mm, $D = (25, 100, 50, 50, 100, 25)$ mm; (a) by Guo and Min (2015); (b) by author's Matlab code	117
4.4	Comparison of sound absorption coefficient of SL-MPP with inhomogeneous perforation and uniform cavity as in Prasetyo et al. (2016) with the homogeneous MPP (Maa, 1975)	119
4.5	Comparison of sound absorption coefficient of SL-iMPP with multi-cavity depth (Author's model), with the homogeneous MPP with uniform cavity depth (Maa, 1975)	120
4.6	Comparison of sound absorption coefficient of SL-iMPP (Author's model) with the homogeneous MPP as in Sakagami et al. (2009a) (both models are with multi-cavity depths)	120
4.7	Effect of perforation ratio on sound absorption coefficient of the single layer inhomogeneous MPP model; $d_1 = 0.8$ mm, $d_2 = 0.4$ mm, and $D_1 = 30$ mm, $D_2 = 40$ mm, $t = 1$ mm; (p_1 varied), (a) $p_2=1\%$, (b) $p_2=2.5\%$, (c) $p_2=4\%$	123

4.8	Effect of perforation ratio on sound absorption coefficient of the single layer inhomogeneous MPP model; $d_1 = 0.8$ mm, $d_2 = 0.4$ mm, and $D_1 = 30$ mm, $D_2 = 40$ mm, $t = 1$ mm; (a) $p_1=0.6\%$, (b) $p_2=1\%$, (c) $p_2=2\%$, (p_2 varied)	124
4.9	Effect of hole diameter on sound absorption coefficient of the single layer inhomogeneous MPP model: $D_1 = 30$ mm, $D_2 = 40$ mm, $p_1 = 0.6\%$, $p_2 = 4\%$, $t = 1$ mm, (d_1 varied), (a) $d_2=0.3$ mm, (b) $d_2=0.4$ mm, (c) $d_2=0.5$ mm, (d) $d_2=0.8$ mm	126
4.10	Effect of hole diameter on sound absorption coefficient of the single layer inhomogeneous MPP model: $D_1 = 30$ mm, $D_2 = 40$ mm, $p_1 = 0.6\%$, $p_2 = 4\%$, $t = 1$ mm, (a) $d_1=0.3$ mm, (b) $d_1=0.4$ mm, (c) $d_1=0.5$ mm, (d) $d_1=0.8$ mm, (d_2 varied)	127
4.11	Illustration of the general features of the inhomogeneous MPP to have an optimum sound absorption performance	128
4.12	Effect of panel thickness variation on the sound absorption coefficient of single layer inhomogeneous MPP; $d_1 = 0.8$ mm, $d_2 = 0.4$ mm; $p_1 = 0.6\%$, $p_2 = 4\%$, and $D_1 = 30$ mm, $D_2 = 40$ mm	130
4.13	Panel thicknesses effects on specific acoustic impedance values (real part) of single layer inhomogeneous MPP; $d_1 = 0.8$ mm, $d_2 = 0.4$ mm; $p_1 = 0.6\%$, $p_2 = 4\%$, and $D_1 = 30$ mm, $D_2 = 40$ mm	130
4.14	Panel thicknesses effects on specific acoustic impedance values (imaginary part) of single layer inhomogeneous MPP; $d_1 = 0.8$ mm, $d_2 = 0.4$ mm; $p_1 = 0.6\%$, $p_2 = 4\%$, and $D_1 = 30$ mm, $D_2 = 40$ mm	131

- 4.15 Effect of the variation of the cavity depth (D_2 varied), on 133
absorption coefficient for a single layer MPP with inhomogeneous
perforation: $d_1 = 0.8$ mm, $d_2 = 0.4$ mm, $p_1 = 0.6\%$, $p_2 = 4\%$, $t = 1$
mm, (a) $D_1=30$ mm, (b) $D_1=40$ mm, (c) $D_1=50$ mm, (d) $D_1=80$ mm
- 4.16 Effect of the variation of the cavity depth (D_1 varied), on 134
absorption coefficient for a single layer MPP with inhomogeneous
perforation: $d_1 = 0.8$ mm, $d_2 = 0.4$ mm, $p_1 = 0.6\%$, $p_2 = 4\%$, $t = 1$
mm, (a) $D_2=30$ mm, (b) $D_2=40$ mm, (c) $D_2=50$ mm, (d) $D_2=70$ mm
- 4.17 Comparison of measured sound absorption coefficient with the 136
theoretical model (Figure 3.3, Equation (3.7) and (3.10)) for
samples listed in Table 3.1: (a) i-MPP-1: $D_1 = 40$ mm, $D_2 = 75$
mm; (b) i-MPP-1: $D_1 = 25$ mm, $D_2 = 55$ mm
- 4.18 Comparison of measured sound absorption coefficient with the 137
theoretical model (Figure 3.3, Equation (3.7) and (3.10)) for
samples listed in Table 3.1: (a) i-MPP-2: $D_1 = 75$ mm, $D_2 = 15$
mm; (b) i-MPP-2: $D_1 = 40$ mm, $D_2 = 75$ mm
- 4.19 Comparison between sound absorption coefficients of the DL- 141
iMPP with and without back cavity partition: iMPP₁: $t_1 = 1$ mm, d_1
 $= 0.6$ mm, $d_2 = 0.3$ mm, $p_1 = 0.6\%$, $p_2 = 3.0\%$ and iMPP₂: $t_2 = 2$
mm, $d_3 = 0.3$ mm, $d_4 = 0.5$ mm, $p_3 = 4.0\%$, $p_4 = 0.2\%$; (a) $D_1 = 20$
mm, $D_2 = 22$ mm, (b) $D_1 = 20$ mm, $D_2 = 32$ mm
- 4.20 Comparison between sound absorption coefficients of the DL- 142
iMPP with and without back cavity partition: iMPP₁: $t_1 = 1$ mm, d_1
 $= 0.9$ mm, $d_2 = 0.4$ mm, $p_1 = 0.6\%$, $p_2 = 3.0\%$ and iMPP₂: $t_2 = 2$

	mm, $d_3 = 0.5$ mm, $d_4=0.3$ mm, $p_3=1.0\%$, $p_4 = 3.5\%$; (a) $D_1 = 20$ mm, $D_2 = 22$ mm, (b) $D_1 = 20$ mm, $D_2 = 32$ mm	
4.21	Comparison between sound absorption coefficients of the DL-iMPP with and without back cavity partition: iMPP ₁ : $t_1 = 1$ mm, $d_1 = 0.9$ mm, $d_2 = 0.3$ mm, $p_1 = 0.8\%$, $p_2 = 2.5\%$ and iMPP ₂ : $t_2 = 2$ mm, $d_3 = 0.3$ mm, $d_4 = 0.8$ mm, $p_3 = 4.0\%$, $p_4 = 1.0\%$; (a) $D_1 = 20$ mm, $D_2 = 22$ mm, (b) $D_1 = 20$ mm, $D_2 = 32$ mm	143
4.22	Schematic diagram of: (1) and (2) SL-iMPP; (3) DL-iMPP combined from the two SL-iMPPs	145
4.23	Comparison of sound absorption coefficient between: (1) SL-iMPP with multi-cavity depth, (Section 3.3), and (2) DL-iMPP with a uniform cavity, (Section 3.4.1)	145
4.24	Schematic diagram of the homogeneous DL-MPP models (Sakagami et al., 2010a) with the DL-iMPP model (author's proposed model as in Section 3.4.1), both models are with uniform cavity depth)	147
4.25	Comparison of absorption coefficients between DL-iMPP with uniform cavity, (author's model as in Section 3.4.1) and the homogeneous DL-MPP (Sakagami et al., 2010a) (cavity depth: $D_1 = 20$ mm, $D_2 = 32$ mm)	149
4.26	Absorption coefficients of inhomogeneous DL-iMPP with varying cavity depth; iMPP ₁ : $t_1 = 0.5$ mm, $d_1 = 0.8$ mm, $d_2 = 0.2$ mm, $p_1 = 0.6\%$, $p_2 = 2.0\%$ and iMPP ₂ : $t_2 = 2$ mm, $d_3 = 0.3$ mm, $d_4 = 0.7$ mm, $p_3 = 3.5\%$, $p_4 = 0.5\%$; (a) D_1 varied, D_2 fixed and (b) D_1 fixed, D_2	151

	varied	
4.27	Comparison of sound absorption coefficient between SL-MPP (Maa, 1998), DL-MPP (Sakagami et al., 2010a), TL-MPP (Sakagami et al., 2014b) with a uniform cavity and the DL-iMPP _{MD} (author's model)	154
4.28	Comparison of sound absorption coefficient between the homogeneous DL-MPP (Qian et al., 2017) and the DL-iMPP _{MD} (author's model). Both models have multiple-cavity depth	156
4.29	Effect of variation of cavity depth between the two iMPPs (D_1) on the sound absorption coefficient of the DL-iMPP _{MD} absorber system. The MPP parameters are: ($d_1, d_2, d_3, d_4 = 0.2, 0.8, 0.4, 0.3$ mm), ($p_1, p_2, p_3, p_4 = 3.0\%, 1.5\%, 1.5\%, 4.0\%$), $t = 0.5$ mm	160
4.30	Effect of variation of cavity depth behind the iMPP ₂ (D_4) on sound absorption coefficient of the DL-iMPP _{MD} : (a) the schematic view, (b) $D_1 = 10$ mm, (c) $D_1 = 20$ mm, (d) $D_1 = 30$ mm. The MPP structural parameters are: $t = 0.5$ mm, ($d_1, d_2, d_3, d_4 = 0.2, 0.8, 0.4, 0.3$ mm), ($p_1, p_2, p_3, p_4 = 3.0\%, 1.5\%, 1.5\%, 4.0\%$)	161
4.31	Effect of variation of cavity depth behind the iMPP ₂ (D_3) on sound absorption coefficient of the DL-iMPP _{MD} : (a) the schematic view, (b) $D_1 = 10$ mm, (c) $D_1 = 20$ mm, (d) $D_1 = 30$ mm. The MPP structural parameters are: $t = 0.5$ mm, ($d_1, d_2, d_3, d_4 = 0.2, 0.8, 0.4, 0.3$ mm), ($p_1, p_2, p_3, p_4 = 3.0\%, 1.5\%, 1.5\%, 4.0\%$)	162
4.32	Comparison between the predicted and measured absorption coefficients of DL-iMPP system (with partition): (a) $D_1 = 10$ mm,	165